

MIT OpenCourseWare
<http://ocw.mit.edu>

8.13-14 Experimental Physics I & II "Junior Lab"
Fall 2007 - Spring 2008

For information about citing these materials or our Terms of Use, visit: <http://ocw.mit.edu/terms>.

The Zeeman Effect and Hyperfine Structure in Mercury

MIT Department of Physics

(Dated: January 31, 2008)

The magnetic splitting of spectral lines. A scanning Fabry-Perot interferometer is used to measure the Zeeman effect in mercury. The results are compared with the expectations derived from the vector model for the addition of atomic and nuclear angular momenta. A value of the ratio e/m of the electron is derived from the data.

PREPARATORY PROBLEMS

1. Draw a diagram that shows the effect of a weak magnetic field on the otherwise degenerate sub-states involved in the transitions which produce the green line (5460.7 Å) and the yellow doublet (5769.6 Å and 5790.7 Å) of mercury. See Melissinos-1966[1], page 334 but beware of the error in the structure diagram for the 5790.7 Å line! Note that there is another (Hg) yellow line at 5789.7 Å but it is quite weak.
2. Derive the Landé g -factors for the states involved in the production of these lines.
3. What would the Zeeman effect be on the 5461 Å line if the gyromagnetic ratio of the electron were 1 instead of 2.001?
4. What is the expected spread in wavenumbers for the hyperfine structure of natural mercury? What is an appropriate spacing of the Fabry-Perot mirrors to acquire this spectrum?
5. Estimate the Doppler width of the 5461 Å line from the mercury lamp and compare it with the expected Zeeman splittings. Assume the temperature of the emitting vapor is 500 K.
6. Derive a formula for e/m in terms of the measured separations of identified peaks in the interferogram of the Zeeman pattern, the distance between the plates of the interferometer, the strength of the magnetic field, and various physical constants.

1. INTRODUCTION

Since Faraday's discovery in 1848 of magnetically induced circular birefringence (the Faraday Effect), the search for effects of electric and magnetic fields on optical phenomena has been pursued with more and more powerful methods of spectroscopy and stronger and stronger fields. In 1862, in his last experimental work, Faraday himself used the most powerful magnet and best prism spectroscope available in an unsuccessful attempt to detect an effect of a magnetic field on the spectral lines emitted by sodium vapor in a Bunsen burner flame. Three decades later Pieter Zeeman in Leyden, unaware

of Faraday's earlier attempt, was induced "by reasons of minor importance" to try to detect a magnetically induced change in the light of a sodium flame [2]. He too failed. However, as Zeeman describes it in his discovery paper of 1896, [3] his attention was subsequently drawn to Maxwell's sketch of Faraday's life in which Faraday's last experiment is mentioned. Zeeman wrote "If a Faraday thought of the possibility of the above mentioned relation, perhaps it might be yet worth while to try the experiment again with the excellent auxiliaries of spectroscopy of the present time." Using a grating ruled on the marvelous engine of Rowland at Johns Hopkins he observed a broadening of the spectral lines emitted by sodium vapor heated in a flame between the poles of a powerful Ruhmkorff magnet which produced a field of 10 kilogauss. Zeeman proposed a theoretical interpretation based on Lorentz's idea that "in all bodies small electrically charged particles with a definite mass are present." Given this concept, the rest of the interpretation is, from a modern point of view, hardly more than a dimensional analysis. Nevertheless this early theory of the "normal" Zeeman effect showed how to interpret the observed line broadening as a measure of e/m , the charge to mass ratio of the electron. The idea was that the frequency of a spectral line emitted by an atom is the frequency of a harmonic vibration of an electron in the atom. Any such vibration can be resolved into two components, one along some particular direction which we take to be the direction of the z axis, and the other in the xy plane. The xy component, in turn, can be represented as the sum of two components of constant amplitude rotating in opposite directions about the z axis. With each such circular component of motion one can associate a central restraining force given by

$$F = mr\omega^2 \quad (1)$$

where ω is the angular frequency and r is the radius of the circular motion. If a magnetic field of magnitude B is now imposed in the z direction, the central force will be either increased or decreased by a perturbing (i.e. small compared to F) Lorentz force of magnitude $\frac{Bewr}{c}$ (cgs units), resulting in a changed frequency of circular motion given by the equation

$$mr(\omega + \Delta\omega)^2 = F \pm \frac{Bewr}{c} \quad (2)$$

or

$$mr[\omega^2 + 2\omega\Delta\omega + (\Delta\omega)^2] = mr\omega^2 \pm \frac{Bewr}{c} \quad (3)$$

Neglecting the $(\omega)^2$ term, one obtains the simple expression

$$\omega + \Delta\omega = \omega \pm \frac{Be}{2mc} \quad (4)$$

for the frequencies of light viewed along the direction of the field (as viewed through a hole bored through the magnet pole piece). In directions perpendicular to the field, one sees both these shifted frequencies and the unshifted frequency of the components of vibration along the z axis which, being parallel to the field, is unaffected. With the resolution available to Zeeman the individual frequency-shifted lines were unresolved. However, Lorentz pointed out to Zeeman that the edges of the broadened lines observed parallel to the field, supposedly being light radiated by charges in right and left circular motions, should exhibit circular polarization in opposite senses with respect to one another. With a quarter wave plate and Nicol prism polarizer Zeeman confirmed the prediction. And by rough estimation of $\Delta\omega$ and knowledge of B he obtained a value of 10^7 esu for e/m .

Within a few months of Zeeman's publication magnetically split lines were spectroscopically resolved and found in many cases to consist of more than the "normal" Zeeman triplet, and to have frequency shifts other than $\pm \frac{Be}{2mc}$. The "anomalous" Zeeman effect, which proved to be the rule and not the exception, defied explanation until the advent of quantum mechanics and the discovery of spin.

A modern understanding of the Zeeman effect can be approached on several levels. The vector model, which you should master before starting the experiment, is explained in [4] and in various texts on quantum mechanics and atomic structure listed in the references. It provides a useful image of the atomic machinery involved in the Zeeman effect and yields accurate predictions of the Zeeman effect in atoms whose excited states can be described according to the LS coupling scheme (Russell-Saunders coupling). Information about the mercury spectrum in general and the Zeeman effect on the green and yellow lines of mercury can also be found in Melissinos. (Beware of errors in Melissinos' description of the hyperfine structure of the mercury lines.) Specially useful references are [5, 6]. Additional background material on the quantum theory of the Zeeman effect can be found in [6–14]. Further details of the physical optics of the interferometer can be found in [15, 16].

2. EXPERIMENTAL ARRANGEMENT

In this experiment you will measure the weak-field Zeeman effect on the green and yellow lines of mercury and by means of a Fabry-Perot interferometer. This device provides the high spectral resolution necessary for the detection and measurement of the small fractional changes in wavelength caused by "weak" magnetic fields of several thousands of gauss. The results reveal some of the important properties of angular momenta, spin, and the dipole

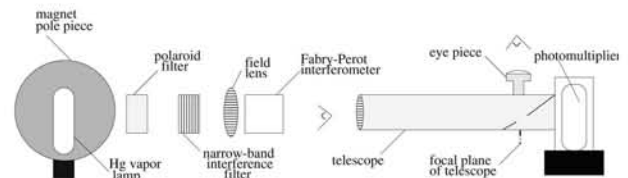


FIG. 1: Schematic diagram of the optical arrangement for recording the intensity at the center of the Fabry-Perot interferogram. The focal length of the collimating field lens is 33 ± 0.5 cm and the focal length of the telescope is 43.5 ± 0.5 cm. The optical height of the Fabry-Perot is 12.2 ± 0.2 cm.

selection rules, as well as an accurate value of e/m from an interpretation of the data based on the vector model for the quantum mechanical addition of angular momentum. In addition, with sufficient care in the adjustment of the apparatus you can detect and measure the hyperfine structure of the green line of the odd isotopes of mercury due to the interactions between the electronic and nuclear magnetic moments, and the spread in wavelength of the lines of the even isotopes due to the differences in the number of neutrons in their nuclei.

The optical arrangement is illustrated in Figure 1. Light emitted by a low-pressure mercury vapor lamp passes through a narrow-band interference filter, an optional Polaroid filter, a field lens, the Fabry-Perot interferometer, and a telescope. When properly aligned this system produces at the focal plane of the telescope objective lens interference fringes in the form of circular rings concentric with the axis. A 45° front-aluminized mirror with a small hole in the aluminization centered on the focal plane reflects most of the ring pattern for viewing through the eyepiece, while allowing the light at the center "bull's eye" of the ring pattern to pass through to the photomultiplier. During a spectrum scan the separation of the Fabry-Perot plates is varied by two or three wavelengths by application of a saw-tooth voltage with an amplitude of several hundred volts to three piezoelectric crystals on which one of the plates is mounted. As the separation decreases (increases) the rings in the image plane expand (contract). A plot of the intensity of light passing through the hole located at the center of the ring pattern against the magnitude of the saw-tooth voltage is, in effect, an ultra-high resolution spectrum over a very narrow range of frequencies.

Figure 2 shows the electronic arrangement for recording the central intensity as a function of the voltage applied to the piezoelectric crystal. The photomultiplier output is fed directly to the Y input of an oscilloscope. A signal equal to the voltage ($\div 100$) applied to the piezoelectric crystals is fed from the interferometer controller to the X input of the digital oscilloscope.

3. PROCEDURE

1. Determine the optimum mirror separation

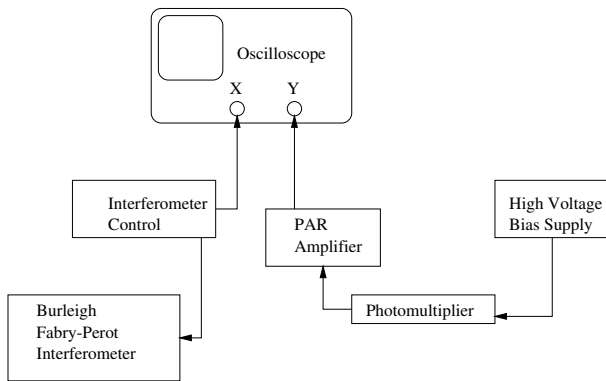


FIG. 2: Schematic diagram of the electronic arrangement for recording the interferogram in the form of a plot of the central intensity versus the separation of the Fabry-Perot plates.

for measurement of the zeeman splittings

Calculate the separation between the Fabry-Perot mirrors which will provide a “free spectral range” suitable for the desired measurements. What you want to avoid is having the extreme red-shifted Zeeman components of a given line in one order of interference overlap the extreme blue-shifted components of the line in the next order when the field is at maximum strength. Estimate the total width of the Zeeman pattern that you expect at the maximum attainable field strength. Calculate the mirror separation which will give you the necessary free spectral range to accommodate this width.

2. **Align the interferometer** The Burleigh Fabry-Perot interferometer is a delicate instrument capable of providing spectrum measurements of extraordinary resolution and precision. Please treat it with the utmost care. In particular, **do not press the mirrors together by turning the micrometer screws too far as you may crack the sapphire blocks on which the micrometer crews press. The ‘zero’ position of the mirrors is when the micrometer nearest the edge of the optical table reads $12.212 \pm 15 \mu\text{m}$.** If you encounter any problems or are uncertain how to adjust the interferometer, call for assistance.

Mount the mercury spectral calibration lamp between the pole pieces, and turn it on using the AC setting at 18mA. Once the lamp discharge has been initiated, it can be run with a DC current greatly reducing the lamp variability. Adjust the collimating lens (plano-convex, focal length = $33 \pm 0.5\text{cm}$) and the position and orientation of the interferometer so that the light falls on the input mirror and the view through the Fabry-Perot mirrors looking toward the lamp is fully illuminated. Put the interference filter for the 5461 \AA green line of mercury in the beam. Begin by adjusting all three micrometers to a setting of 15mm. The micrometers have

a range of 25mm where the smallest division on the micrometer shaft corresponds to $10 \mu\text{m}$.

Coarse Alignment of the Fabry-Perot ATTENTION: *Do not look through the interferometer towards the laser. All alignment should be done while viewing the notecard from above the experimental setup.*

This section is only needed if the interferometer is so poorly aligned that you do not see any circular interference pattern at the output of the Fabry-Perot after turning on the lamp.

A quick method for course alignment of the Fabry-Perot interferometer is easily accomplished using a laser. Arrange a helium-neon laser to pass through the interferometer mirrors as close to on-axis as possible. Place a white piece of paper a few inches away from the output of the F-P and note the pattern of spots observed. Under coarse alignment, the spots will appear to ‘walk’ off the card indicating that the mirrors are NOT parallel. Adjustments to the micrometers should be made to cause these helium-neon spots to become more numerous and concentrated (indicating better and better parallelism of the mirrors) until they appear to collapse onto a single point at which point fringing should appear.

Now, by making small adjustments and taking careful notes on their effects, make the mirrors parallel by adjusting two of the three micrometers while viewing the light coming through the Fabry-Perot mirrors. When coarsely adjusted, you may only see ‘arcs’ of the interference patterns. As the mirrors are nearly parallel you will see many narrow circular fringes. Fine adjustment will produce comparatively large, sharp circular fringes concentric with the center of your field of view and separated by dark gaps with fainter and narrower rings. When the mirrors are perfectly parallel the circular fringes are sharp and do not change in diameter as you move your eye back-and-forth, and up-and-down.

3. **Align the telescope** Check that the mirror mounted inside the telescope under the eyepiece is inclined at an angle of 45° so that it reflects the light from the telescope lens into the eyepiece. Adjust this angle using the silver screw from the bottom of the assembly. Focus the eyepiece on the tiny aperture (a ragged laser-drilled hole in the aluminization near the center of the mirror). Then point the telescope at a distant object and focus it by adjusting the slide tube.

Place the telescope so that the light emerging from the interferometer enters the objective lens (focal length = $43.5 \pm 0.5\text{cm}$). (Leave sufficient room between the telescope and the interferometer to insert your head for direct viewing of the interference fringes). Adjust the orientation of the telescope so

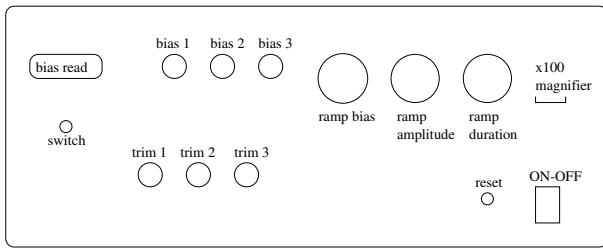


FIG. 3: Diagram of the front panel of the interferometer controller. Note that the knobs are friction-coupled to their shafts so that they turn past the zero and maximum positions without harm.

that the circular fringes seen through the eyepiece are concentric with the tiny aperture in the 45° mirror. (The broad rings are successive orders of interference of the light from the even isotopes of mercury: the breadth of the line is due to the effect of the spread in mass of the isotopes. The faint, narrow rings between the broad ones are the hyperfine lines of the odd isotopes, separated slightly in wavelength from the others as a result of the interaction between the nuclear and electronic magnetic moments.)

4. **Adjust the fabry-perot controller** Turn on the controller and explore its operation with the help of the diagram in Figure 3 and the instrument manual. The function of the controller is to supply a sawtooth voltage to each of three piezoelectric crystals on which the input (left) Fabry-Perot mirror is mounted. The duration and amplitude of the sawtooth voltages are controlled by the correspondingly labeled knobs. The ramp bias knob controls the voltage level of the midpoint of the scan voltage applied to all three crystals; the three bias controls on the left adjust the mean voltages applied to each crystal. The trim controls adjust the slopes of the sawtooth voltages to compensate for any differences that may exist in the electromechanical properties of the crystals. Start with each of the trim controls in their most counterclockwise position.

With the ramp amplitude turned to zero, set the three bias controls and the three trim controls to near their middle values (~ 250 V). Application of the bias voltages to the piezoelectric crystal mounts of the input mirror will disturb the parallelism. So, once again, view the fringes directly with your eye close to the output mirror of the interferometer and make the mirrors parallel by adjusting the bottom and top right micrometers. Now view the fringe pattern through the telescope and tweak the bias controls for maximum sharpness. Adjust the telescope orientation so that the aperture hole is exactly at the bull's eye of the circular fringe pattern. You can shift the fringe pattern by adjusting the ramp bias control.

5. **Acquire the spectrum** Put the photomultiplier in its place at the end of the telescope and turn up the Photomultiplier high voltage to ≈ -1000 v. Feed the signal from the photomultiplier tube (PMT) to the voltage preamplifier with the low frequency (LF) roll off control set to DC, and the high frequency (HF) roll off set to a value that satisfactorily reduces the vertical jitter due to electronic noise without suppressing the fine features of the spectrum. Display the output on the y-axis of the digital oscilloscope with the scan signal from the Fabry-Perot controller connected to the x-input. Adjust the scan amplitude so that the piezoelectric drive is activated. Select a bias sweep amplitude and repetition rate that produces a pleasing display of the variation of light intensity at the bullseye of the interferometer pattern over a range of two or three free spectral ranges. Adjust the three bias controls to maximize the amplitudes of the peaks.

Observe the pattern and identify the hyperfine lines with the help of the plot copied from the American Institute of Physics Handbook and posted on the wall.

6. **Trial Runs** The magnet is capable of producing a field of ~ 9.4 kG at a current of 50A. **Please do not exceed this current level!** As a result of such high currents, the magnet coils must be cooled during operation. A Neslab chilled-water circulator (under the left-hand side of the optical table) is installed for this purpose. Turn on the Neslab as soon as you begin your lab sessions to allow time for the water to be cooled. The power switch is on the top left-hand side of the unit. Once the water is circulating, you can turn on the magnet power supply (located under the table), making sure that the current level is at the lowest possible setting.

When everything is properly adjusted, with the bull's eye of the interference pattern centered on the hole in the 45° mirror and with the bull's eye intensity signal displayed on the oscilloscope, a pattern similar to that in Figures 4 and 7 with $R \approx 0.9$ should be seen.

Observe the fringe pattern through the telescope as you increase the magnet current. Note the behavior of the hyperfine lines. Test the effect on the fringe pattern of inserting a Polaroid filter in the optical path between the source lamp and the Fabry-Perot. Rotate the Polaroid and figure out what is happening. (You can determine the transmission axis of the Polaroid filter by observing light reflected at small angles of grazing incidence from any non-metallic glossy surface like that of the table in the next room.)

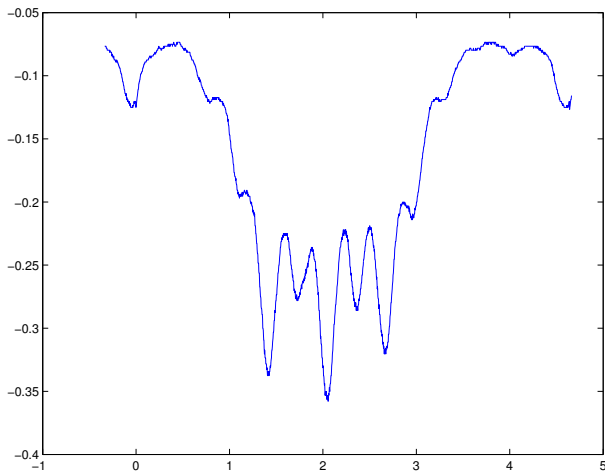


FIG. 4: Sample interferogram of the 5461 Å line of mercury. Magnet current = 50A \sim 0.94T. The amplifier gain = 1000 and the PMT bias = -900 VDC. The units of the x-axis are seconds and of the y-axis are volts.

4. QUANTITIES YOU WILL DETERMINE

1. The Zeeman splittings of the green 5461 Å and yellow 5770 Å and 5791 Å lines of mercury.
2. The Landé g-factors for the levels involved in the mercury lines.
3. The value of e/m for the electron.
4. The hyperfine structure of the mercury 5461 Å line.
5. The isotope shift (effect of nuclear mass) of the 5461 Å lines of the even isotopes of mercury.

4.1. The green line of mercury

Using the Hall probe magnetometer explore and record, as a function of the supply current, the intensity of the field between the pole pieces of the magnet in the region that will be occupied by the mercury vapor and up against the centers of the faces of the pole pieces. (Check the Hall magnetometer zero setting by inserting the probe into the magnetically shielded cavity provided, and check the calibration with the 5 kilogauss standard magnet, also provided.)

A convenient way to measure the Zeeman splittings is to record the digital reading of the ramp bias required to move the various interference rings seen in the telescope to a chosen fiducial position marked by a dirt spot on the 45° mirror at the focal plane of the telescope. To do this first stop the scanning action by turning the ramp amplitude to zero. Then select a dirt spot on the mirror at some as your fiducial marker. Adjust the ramp bias control so the spot is on the center line of an interference ring of a particular reference spectrum line, and

record the bias reading. Repeat for the other rings of the same order of interference for the spectrum lines whose wavelength shift relative to the reference line you wish to measure. Also record the bias readings for interference rings in several adjacent orders to establish the calibration scale and to provide redundant data from which the random measurement errors can be evaluated.

At zero field tweak up the performance of the interferometer with the bias controls to sharpen up as much as you can the hyperfine components of the green line which appear as the faint, sharper rings between the bright, broad rings of the unresolved emission from the even isotopes. Increase the gain of the oscilloscope y-input to make the hyperfine peaks large enough to be accurately measurable. Here again you can obtain the necessary measurements using the ramp bias control. Beware of confusing interference rings of different orders.

4.2. The yellow doublet of mercury

To observe the mercury yellow lines remove the green interference filter from the optical path and insert the yellow interference filter centered at 5770 Å. Note that there will now be two sets of interference rings present since the filter passes both of the yellow lines. With luck the two sets of rings may be conveniently spaced so that their Zeeman patterns do not overlap at moderate fields. If not, you will have to change the spacing of the mirrors slightly.

Measure the structure and splitting of both components of the mercury yellow doublet. This will require special care because of possible overlapping of the two interference patterns at high field values. Note the slight difference in the Zeeman patterns of the 5769.6 Å and 5461 Å lines. How do they differ and why? A beautiful photograph of the doublet is shown in Fig. 5.

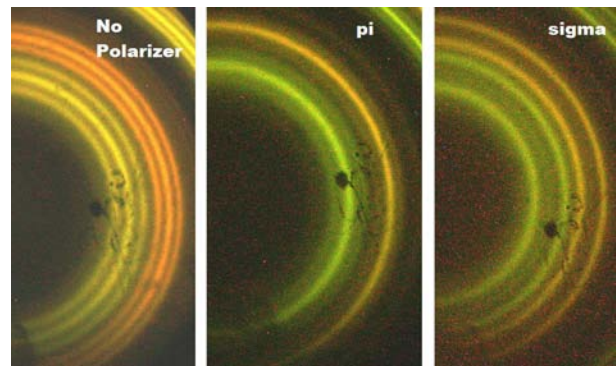


FIG. 5: Photograph of the yellow mercury doublet at 5769.6 and 5790.7 Å showing σ and π transitions. Taken by Matthew Heine and Sarah Trowbridge in 2007. Used with permission.

5. ANALYSIS

To check the results of your ramp bias measurements of the Zeeman splittings you can measure the separations between the peaks of the interferograms utilizing Matlab and fitting the peak locations. **Be sure to measure the separation between the same Zeeman components in adjacent orders**, i.e. the distance in interferogram corresponding to the free spectral range. From these quantities and the separation of the mirrors of the Fabry-Perot interferometer, compute the effective dispersion of the spectroscopy, i.e. the shift in wave number per unit distance on the photographs.

1. Tabulate all the measured frequency shifts in units of wave numbers $\frac{\Delta f}{c} = \Delta \frac{1}{\lambda}$ per kilogauss, e.g. $(0.1234 \pm 0.012) \text{cm}^{-1} \text{kgauss}^{-1}$.
2. Construct energy level diagrams of the mercury transitions and identify the observed Zeeman component frequencies with the various allowed transitions between the magnetic substates.
3. Measure the hyperfine lines, and identify them with the help of the discussion by Steinfeld (1986).
4. Measure the full width at half maximum of a strong hyperfine line to obtain a measure of the effective resolution of the spectrometry. Measure the FWHM of the bright, unresolved composite line of the even isotopes. Derive from these data a measure of the spread in wavelengths of the even isotope lines due to the differences in their nuclear masses. Can you think of a way to make an order of magnitude theoretical prediction of this spread?
5. Compute the Landé g-factors for the upper and lower states involved in the various transitions (Hg 5461 Å, Hg 5770-5790 Å and the magnetic moments of each of the levels in units of the Bohr magneton.
6. If everything makes sense, i.e. all the measured shifts of the π and σ components are consistent with expectations derived from the vector model and selection rules, then determine a best value for e/m for the entire data set.
7. Estimate the random and systematic errors associated with each of your final quantitative conclusions.

5.1. Possible Theoretical Topics

1. The vector model and the Landé g-factor.
2. Hyperfine structure.
3. The isotope shift.
4. Theory of multi-wave interference in the Fabry-Perot interferometer.

6. THEORY OF THE FABRY-PEROT INTERFEROMETER

A Fabry-Perot interferometer consists of two precisely parallel glass plates with optically flat and highly reflective surfaces facing one another, as illustrated in Figure 6. To use it as a spectrometer one must have, in addition, a lens to focus parallel rays to a point in its image plane and a magnifying eyepiece for examining the intensity pattern of light in the focal plane, i.e. a telescope.

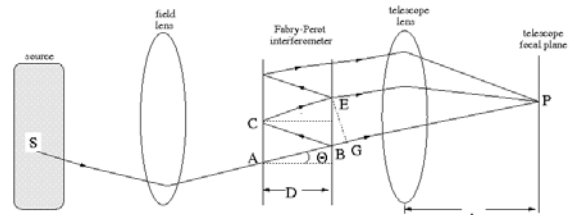


FIG. 6: Geometrical optics of the Fabry-Perot interferometer. Only one of many multiply reflected paths is shown.

Consider a ray of light of wavelength λ emitted by an excited mercury atom at S and making an angle θ with the axis, is incident on the Fabry-Perot from the left at the point A . It will be partially transmitted at each of the two Fabry-Perot mirror surfaces, and will arrive at P after passing through the telescope lens. The portion of the ray reflected at B will be reflected again at C and partially transmitted at E . It will enter the telescope lens parallel to the original ray and will be focussed to the same point P after having traversed an additional distance $2D\cos\theta$. If this additional distance is an integer number of wavelengths, i.e.,

$$2D\cos\theta = m\lambda \quad (5)$$

then the two rays (and all the additional multiply reflected rays) will interfere constructively when brought to the focus at P . Constructive interference among all the multiply reflected rays passing through the interferometer at an angle θ to the axis will produce a circle of interference maxima in the focal plane, i.e., a bright ring of the m th order of interference. If the separation of the plates is increased, then the angular radius of the m th order ring will expand so that the decrease in $\cos\theta$ compensates for the increase in D .

Suppose you want to measure the difference $\delta\lambda$ between two wavelengths very close together, e.g., the wavelength shift between two lines in a Zeeman pattern. Suppose, further, that the average wavelength λ of the two lines is already known to good accuracy. Viewing the light emerging from the interferometer with your naked eye or through a telescope focused on infinity, you will see two concentric sets of interference rings, corresponding to the two wavelengths. Suppose the m th order ring of wavelength λ_1 coincides with a fiducial mark fixed in

the focal plane (e.g. a dirt spot on the 45° mirror in the Junior Lab setup). Call δD the change in mirror separation required to bring the m th order ring of wavelength $\lambda_1 + \delta\lambda$ into coincidence with the fiducial mark. According to equation 5

$$\delta D = \frac{m\delta\lambda}{2\cos\theta} \quad (6)$$

Call ΔD the change in mirror separation required to bring the $m + 1$ ring of wavelength λ_1 into coincidence with the same fiducial mark. In this case

$$\Delta D = \frac{\lambda_1}{2\cos\theta} \quad (7)$$

Combining equation 5, equation 6, and equation 7 and setting $\cos\theta = 1$ (an accurate approximation since $\theta \ll 1$) we obtain

$$\delta\lambda = \lambda \frac{\lambda}{2D} \frac{\delta D}{\Delta D} \quad (8)$$

which is an expression for the desired wavelength difference in terms of the known wavelength λ , the mirror separation D and the ratio of the changes in separation of the mirrors. In practice the changes can be measured as differences in the digital readings of the bias meter on the Burleigh controller. Since the latter are proportional to the actual changes in mirror separation, the ratio of the meter differences is equal to the ratio of the actual separation changes.

From equation 8 one can see that if $\delta\lambda = \lambda \frac{\lambda}{2D} = \frac{\lambda}{m}$, then $\delta D = \Delta D$, i.e., the mirror movement required to shift the ring pattern from the m th order ring of wavelength λ to the m th order ring of wavelength $\lambda + \delta\lambda$ would be the same as the movement required to shift the m th order ring of λ to the m th+1 order of the same wavelength. The quantity $\frac{\lambda}{m}$ is called the free spectral range of the instrument for a particular separation of the mirrors. It represents the difference between two wavelengths such that the m th interference maximum of the larger wavelength coincides with the $(m + 1)$ maximum of the smaller wavelength, i.e. $(m + 1)\lambda = m(\lambda + \frac{\lambda}{m})$. To avoid confusion as to which interference order a given feature of a complex line may belong, it is generally wise to adopt a mirror separation that gives a free spectral range larger than the wavelength difference to be measured.

The effectiveness of a Fabry-Perot interferometer for high-resolution spectroscopy depends critically on the reflectivity of its mirrors - the higher the reflectivity the sharper, or narrower, the lines. To quantify this relation one must consider the combined effects of the reflection coefficient and additional path length on the contribution that each transmitted beam makes to the total complex amplitude of the optical disturbance at P. If we call r the amplitude reflection coefficient, then the factor by which

the amplitude of the ray emerging at E is reduced relative to the direct ray is r^2 . In addition the ray is retarded in phase by the angle

$$\alpha = \frac{2\pi D}{\lambda} \cos\theta \quad (9)$$

Similarly, the n th multiply reflected ray will arrive at P attenuated by the factor $(r^2)^n$ and retarded in phase by $n\alpha$. If the amplitude at P of the wave arriving by the direct path is $Ae^{j(\omega t + \phi)}$, then the total amplitude at P is the complex quantity

$$A_{tot} = Ae^{j(\omega t + \phi)} \left(1 + r^2 e^{-j\alpha} + \left[r^2 e^{-j\alpha} \right]^2 + \left[r^2 e^{-j\alpha} \right]^3 + \dots \right) \quad (10)$$

This is a geometric series of which the sum is

$$A_{tot} = \frac{Ae^{j(\omega t + \phi)}}{1 - r^2 e^{-j\alpha}} \quad (11)$$

The intensity at P is proportional to the square of the magnitude of A_{tot} which we obtain by multiplying A_{tot} by its complex conjugate. The ratio of this intensity to the intensity at the center where $\theta = 0$ is then

$$\frac{I}{I_0} = \frac{(1 - R)^2}{1 - 2R\cos\alpha + R^2} \quad (12)$$

where we have replaced r^2 by R , the intensity reflectivity of the surfaces. At any fixed wavelength and plate separation, α depends only on the position of P in the focal plane of the telescope lens and not on the position of S. Thus the ratio of the sum of the contributions to the intensity at P from all the incoherent atomic sources in the lamp to the sum at the center of the focused ring pattern is given by equation 12 which is, therefore, the general formula for the intensity in the focal plane.

The maxima of the intensity occur where $\frac{\alpha}{2\pi} = \frac{2D}{\lambda} \cos\theta = m$, where m is an integer called the order of the interference. Changes in the value of $\frac{\alpha}{2\pi}$ are related to changes in D , λ , and θ by the differential relation

$$\delta\left(\frac{\alpha}{2\pi}\right) = \frac{2\cos\theta}{\lambda} \delta D - \frac{2D\cos\theta}{\lambda^2} \delta\lambda - \frac{2D\sin\theta}{\lambda} \delta\theta \quad (13)$$

At the center (bull's eye) of the interference ring pattern, where $\cos\theta = 1$, the order of interference can be changed from m to $m + 1$ either by increasing D by $\Delta D = \lambda/2$ or by decreasing λ by $\Delta\lambda = \lambda \frac{\lambda}{2D} = \frac{\lambda}{m}$. As mentioned previously, quantity $\Delta\lambda$ is called the free spectral range. It is the maximum width of the Zeeman pattern of a given order of interference that can be displayed without overlapping the patterns of the adjacent orders. To express the free spectral range in terms of wave numbers (reciprocal wavelength) one uses the relation

$$|\Delta(\frac{1}{\lambda})| \approx \frac{1}{\lambda^2} \Delta\lambda = \frac{1}{2D} \quad (14)$$

In a typical setup $D \approx 0.25\text{cm}$, $\lambda \approx 5000 \text{ \AA}$, $m \approx 10,000$, and the free spectral range in wave numbers is $\frac{1}{2D} = 2.0 \text{ cm}^{-1}$.

To see what equation 12 tells about how the intensity depends on very small displacements of the plates and on very small changes of the wavelength, we define two dimensionless parameters f and g such that $D = (1+f)m_0\lambda_0/2$ and $\lambda = (1+g)\lambda_0$. The parameter f measures the change in separation of the plates in units of $\frac{\lambda_0}{2}$ and is of the order of $\frac{1}{m_0}$. We will be interested in the effects of very small changes in wavelength for which typical values of g are also of the order $\frac{1}{m_0}$ so that $\frac{1}{1+g}$ can be approximated to high accuracy by $(1-g)$. In practical setups $\theta < 1^\circ$ so that we can replace $\cos\theta$ by the approximation $1 - \frac{\theta^2}{2}$. Substituting the expressions for D and λ with these approximations in equation 12 and dropping the terms of negligible smallness, we obtain

$$\frac{I}{I_0} = \frac{(1-R)^2}{1 - 2R\cos\left[\pi m_0(1+f)(1-g)(1 - \frac{\theta^2}{2})\right] + R^2} \quad (15)$$

Figure 7 is a plot of the intensity versus angle in the interferograms formed by a Fabry-Perot with $m_0 = 24,818$ and $R = 0.8$, illuminated by light with two wavelengths, $\lambda_1 = 5461 \text{ \AA}$ and $\lambda_2 = \lambda_1(1 + 5 \times 10^{-6})$. The four sets of curves are for four different values of the plate separation. The dashed lines are the separate intensity curves for the two wavelengths, and the solid line is their sum. Figure 8 shows the summed intensities versus angle for the same Fabry-Perot and wavelengths, but for four different reflectivities.

Figure 9 shows plots of the intensity at the center of the interferogram $\theta = 0$ as functions of the plate separation for four reflectivities. This is the form of the interferogram/spectrogram you will record in the present experiment.

The intensity function has maxima in the focal plane on concentric circles to which are focused rays leaving the Fabry-Perot at angles θ such that $\frac{2D}{\lambda}\cos\theta = m$, where m is an integer. Since we are dealing with small angles we again use the approximation $\cos\theta \approx 1 - \frac{\theta^2}{2}$. If $\frac{2D}{\lambda} = m_0$, the m th maximum will lie at the angles $\theta_m = \sqrt{\frac{2(m_0-m)}{m_0}}$.

We now ask "By how much must the phase factor $\alpha = \frac{4\pi D}{\lambda}\cos\theta$ change to decrease the intensity from a maximum value to half maximum?". Remembering that at a maximum the phase factor is an integral multiple of 2π , and using the identity $\cos(2\pi n + \delta\alpha) = \cos(\delta\alpha)$, we have from equation 12 the relation

$$\frac{(1-R)^2}{1 - 2R\cos(\delta\alpha) + R^2} = \frac{1}{2} \quad (16)$$

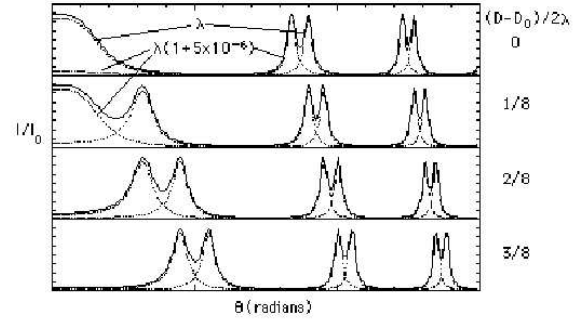


FIG. 7: Plot of intensity against angle in theoretical interferograms of two wavelengths differing in wavelength by 5 parts in a million produced by a Fabry-Perot with $\frac{2D_0}{\lambda_0} = 24,818$, and reflectivity $R=0.8$. The four plots are for four successively larger plate separations, the first differing from the fourth by $\frac{3}{8}$.

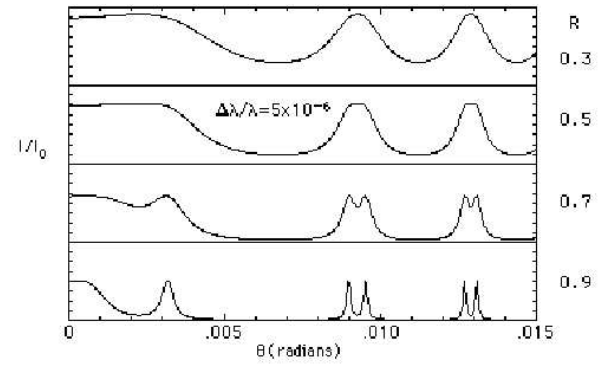


FIG. 8: Plot of intensity against angle in interferograms of light containing two wavelengths, for various reflectivities.

from which we obtain

$$\cos(\delta\alpha) = 1 - \frac{(1-R)^2}{2R} \quad (17)$$

or, to a good approximation

$$\delta\alpha = \frac{1-R}{\sqrt{R}} \quad (18)$$

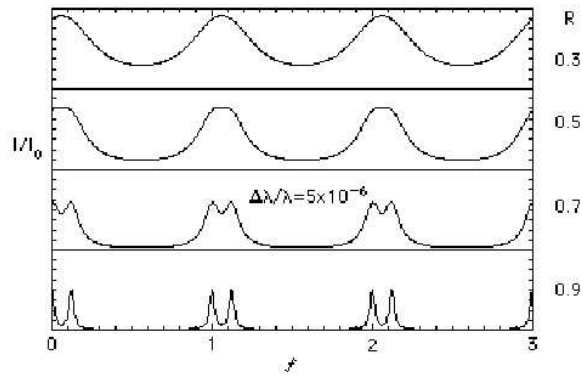


FIG. 9: Plot of intensity at the center of the interferogram against the separation of the FP mirrors for various reflectivities.

If we measure the intensity at $\theta = 0$ as a function of the separation, then the change in D to the half intensity point is

$$\delta D = \frac{\lambda}{4\pi} \frac{1-R}{\sqrt{R}} \quad (19)$$

The change in D between successive maxima is $\frac{\lambda}{2}$. Thus the resolution of the interferometer, defined as the ratio of these quantities and called the finesse, is

$$finesse = \frac{2\pi\sqrt{R}}{1-R} \quad (20)$$

-
- [1] A. Melissinos, *Experiments in Modern Physics* (Academic Press, 1966).
 - [2] *Pieter Zeeman's Nobel Prize Lecture* (1902).
 - [3] P. Zeeman, *Phil. Mag* **43**, 226 (1897).
 - [4] A. Melissinos, *Experiments in Modern Physics* (Academic Press, 2003), ISBN QC33.M523, physics Department Reading Room.
 - [5] H. E. White, *Introduction to Atomic Spectra* (McGraw-Hill, 1934), physics Department Reading Room.
 - [6] J. Steinfeld, *Molecules and Radiation* (MIT Press, 1986), ISBN QC454.M6.S83, physics Department Reading Room.
 - [7] S. Gasiorowicz, *Quantum Physics* (John Wiley, 1996), 2nd ed., physics Department Reading Room.
 - [8] E.U. Condon and G. Shortley, *The Theory of Atomic Spectra* (Cambridge, 1959), ISBN QC454.C746, physics Department Reading Room.
 - [9] L. Landau and E. Lifshitz, *Quantum Mechanics* (Pergamon, 1974).
 - [10] E. Merzbacher, *Quantum Mechanics* (Wiley, 1961), ISBN QC174.1.M577, science Library Stacks.
 - [11] E. K. F.K. Richtmyer and T. Lauritsen, *Introduction to Modern Physics* (McGraw-Hill, 1955), ISBN QC21.R537, physics Department Reading Room.
 - [12] H. Semat, *Introduction to Atomic and Nuclear Physics* (Holt Rinehart and Winston, 1962), ISBN QC173.S469, physics Department Reading Room.
 - [13] G. Herzberg, *Phil. Mag* pp. 82–113 (1944).
 - [14] H. Schuler and E. Jones, *Zeitschrift Fur Physik* pp. 630–646 (1932).
 - [15] E. Hecht, *Optics* (Addison-Wesley, 2002), 4th ed., physics Department Reading Room.
 - [16] B. B. Rossi, *Optics* (Addison-Wesley, 1957), ISBN QC355.R831, physics Department Reading Room.